*Article*

# Sustainable PEG-Incorporated Membranes Derived from Expanded Polystyrene Waste for Efficient Microalgae Separation

**Diah Mahmuda [1], Ikhsan Nur Khafifi [1], Budi Arifvianto [1,2], Tutik Sriani [3], Gunawan Setia Prihandana [4,5], Ario Sunar Baskoro [6], Norihisa Miki [7], Muslim Mahardika [1,*]**

[1] Department of Mechanical and Industrial Engineering, Faculty of Engineering, Universitas Gadjah Mada, Yogyakarta 55281, Indonesia; diahmahmuda1989@mail.ugm.ac.id (DM); ikshan.nur.khafifi@mail.ugm.ac.id (INK); budi.arif@ugm.ac.id (BA)

[2] Centre for Innovation of Medical Equipment and Devices (CIMEDs), Faculty of Engineering, Universitas Gadjah Mada, Yogyakarta 55281, Indonesia

[3] Department of Research and Development, PT Global Meditek Utama-IITOYA, Yogyakarta 55581, Indonesia; tsriani@iitoya.com (TS)

[4] Department of Industrial Engineering, Faculty of Advanced Technology and Multidiscipline, Universitas Airlangga, Surabaya 60115, Indonesia; gunawan.prihandana@ftmm.unair.ac.id (GSP)

[5] Research Group of Industrial Management, System Engineering & Manufacturing, Universitas Airlangga, Surabaya 60115, Indonesia

[6] Department of Mechanical Engineering, Faculty of Engineering, Universitas Indonesia, Depok 16424, Indonesia; ario@eng.ui.ac.id (ASB)

[7] Department of Mechanical Engineering, Keio University, Kanagawa 223-8522, Japan; miki@mech.keio.ac.jp (NM)

* Correspondence: Muslim Mahardika, Email: muslim_mahardika@ugm.ac.id.

## ABSTRACT

The production of expanded polystyrene (EPS) continues to increase due to its widespread use, particularly in single-use food packaging, while its extremely slow degradation in landfills contributes to persistent environmental problems. In this study, EPS waste was recycled into functional flat-sheet membranes for microalgae separation as part of a potential wastewater treatment application. To improve membrane structure and performance, polyethylene glycol (PEG) was incorporated into the EPS casting solution as a hydrophilic additive. A series of membranes containing 0–20 wt.% PEG were fabricated via nonsolvent-induced phase separation (NIPS). PEG incorporation altered the membrane morphology, reduced the water contact angle from 100.3° to 85.94°, and increased the pure water flux, with the highest value of 283.13 L $m^{-2}$ $h^{-1}$ obtained for the membrane containing 20 wt.% PEG. Mechanical performance was also improved relative to the pristine EPS membrane, with the highest tensile strength observed at 15 wt.%. Additional thickness, porosity, and mean pore size data confirmed that PEG promoted more extensive pore development during phase inversion. Importantly, both



Received: 26 Dec 2025
Accepted: 19 May 2026
Published: 26 May 2026

pristine and PEG-modified membranes maintained near-complete microalgae rejection (≥99%) under all tested conditions, showing that the permeability enhancement was achieved without a measurable loss of separation performance. Moreover, EPS/PEG membranes showed improved flux recovery after microalgae filtration, with the highest FRR 93 ± 8.9% observed for EPS/PEG-15, suggesting improved fouling reversibility. These findings demonstrate a simple and promising waste-valorization route for converting EPS waste into functional membranes suitable for efficient microalgae separation.

**KEYWORDS**: EPS waste; PEG modification; upcycled membrane; microalgae separation

## INTRODUCTION

Styrofoam is primarily produced from polystyrene, a widely used thermoplastic known for its lightweight nature, thermal insulation, and low production costs [1,2]. Although “Styrofoam” is technically a trademark of Dow Chemical [3], foamed polystyrene materials used in disposable food packaging and protective applications are generally referred to as expanded polystyrene (EPS). Owing to these favorable properties, EPS has been extensively used in disposable plates and cups, electronic packaging, and chemical storage containers, and other short-lifetime applications [4]. However, the continued increase in EPS consumption has created a serious environmental challenge. Because of its very slow degradation rate, discarded EPS ends up in landfills and the wider environment, generating persistent ecological and health concerns [5].

To reduce this burden, various recycling and upcycling approaches have been explored. Thermal and catalytic decomposition are among the most widely reported methods for converting EPS into gases, oils, and monomers that can be reused as chemical feedstocks or alternative fuels [6]. Nevertheless, these methods are often energy-intensive, economically demanding, and may generate harmful pollutants and microplastics, which in turn pose risks to human health and aquatic ecosystems [7]. Recent findings showing that microplastics can alter microbially mediated carbon metabolism in mangrove ecosystems further emphasize that the impact of EPS waste extends beyond its simple physical accumulation [8]. These limitations suggest that, although conventional recycling routes can reduce EPS volume, they do not necessarily provide a simple and sustainable pathway to high-value functional materials.

Accordingly, increasing attention has been directed toward the valorization of EPS waste into more useful products. Previous studies have incorporated post-consumer EPS into waterproofing paint formulations [9], blended it with gasoline to produce construction mortar [10], combined it with a phase-change coating derived from waste cooking oil

[11], and dissolved it in acetone for conversion into fibers and nonwoven fabrics [12]. While these efforts demonstrated the feasibility of transforming EPS waste into value-added materials, most of them are not designed for separation applications and therefore do not address the growing need for sustainable functional materials in water and wastewater treatment. In this regard, the conversion of EPS waste into membrane materials represents a more application-oriented upcycling strategy, since it links plastic waste valorization with the development of separation media for environmental processes.

In the field of membrane technology, several researchers have explored the use of recycled EPS for water treatment applications. Sihombing et al. (2022) [13] fabricated membranes by electrospinning polystyrene with natural zeolite for desalination. Although electrospinning can generate highly porous fibrous structures, it is associated with relatively high energy consumption, limited production throughput, and complex operational requirements, including the need for a high-voltage power supply and strict control of processing conditions [14]. In addition, electrospun membranes often suffer from insufficient mechanical stability, which may restrict their practical applicability [15]. By comparison, phase inversion offers a simpler and more scalable route for membrane fabrication, with better potential for real-world implementation.

Sriani et al. demonstrated the preparation of EPS-based membranes via wet phase inversion for microplastic removal from aquatic environments [16]. Their results confirmed the feasibility of producing recycled EPS membranes with good separation performance. More broadly, phase inversion is well known for enabling improved membrane uniformity and tunable pore structure [17], features that are highly desirable in filtration systems requiring controlled transport characteristics [18]. At the same time, membrane performance achieved by phase inversion still depends strongly on the casting solution composition, and the direct use of EPS as the main polymer matrix does not automatically overcome its intrinsic material limitations. Therefore, further modification remains necessary to improve the practical performance of EPS-derived membranes [19].

One of the main limitations of EPS membranes is their inherent hydrophobicity, which can reduce wettability and hinder water transport across the membrane [20]. In addition, the relatively brittle nature of EPS-derived materials may adversely affect membrane robustness during handling and use. These characteristics limit the broader applicability of recycled EPS as a membrane precursor and indicate that structural or surface modification is required to make such membranes more suitable for aqueous separation processes. Thus, the challenge is not merely to fabricate membranes from EPS waste, but to tailor their properties so that the resulting materials can function effectively in water-based filtration applications [21].

A common strategy to improve membrane performance is the incorporation of additives into the dope solution. Various compounds, including polyvinylpyrrolidone (PVP) [22,23], ethylene glycol, diethylene glycol, and polyethylene glycol (PEG) [24,25] have been reported to enhance membrane characteristics. Among these additives, PEG is particularly relevant to the present study because it can directly address the low wettability of EPS-derived membranes. PEG, also known as macrogol, is a hydrophilic polymer synthesized from ethylene oxide [26,27] and has been widely used to modify membrane morphology and transport properties. Yue et al. reported that PEG modification effectively improved membrane porosity [28]. PEG also possesses good dispersibility and hydrophilicity and is less prone to agglomeration in polymer solutions. Furthermore, the molecular weight of PEG plays an important role in determining membrane characteristics, including pore structure, permeability, and mechanical stability [29]. In particular, low-molecular-weight PEG such as PEG-400 tends to diffuse more rapidly during phase inversion, thereby accelerating solvent-nonsolvent exchange and supporting the development of a more open membrane structure [30]. These characteristics make PEG a promising additive for tailoring the structure and filtration-related properties of EPS-based membranes.

Although PEG has been widely used as a membrane additive in conventional polymer systems, its application in recycled EPS-based membranes remains limited, particularly for microalgae separation. This is an important issue because microalgae are widely used in pharmaceutical, cosmetic, and nutraceutical applications, yet their small particle size and dilute suspension conditions make downstream separation technically challenging and often energy-intensive when conventional techniques such as centrifugation are applied [31]. In this regard, membrane technology offers a promising alternative due to its high separation efficiency, operational ease, scalability, lower chemical consumption, and environmental sustainability [32]. However, for such applications, the membrane materials must exhibit suitable wettability, permeability, and structural stability, which remain challenging for EPS-derived membranes because of their intrinsic hydrophobicity.

Accordingly, this study investigates whether PEG incorporation can improve the wettability, permeability, and mechanical characteristics of recycled EPS membranes without compromising their microalgae rejection performance. To this end, flat-sheet EPS membranes were fabricated via nonsolvent-induced phase separation (NIPS) with different PEG-400 contents in the casting solution. The effects of PEG on membrane morphology, hydrophilicity, mechanical behavior, pure water flux, and microalgae separation performance were systematically evaluated. By combining EPS waste upcycling with PEG-assisted membrane modification in a microalgae filtration context, this work provides insight into the feasibility of producing functional separation membranes from discarded plastics through a simple and potentially scalable approach.

## MATERIALS AND METHODS

### Materials

All chemicals used in this study were purchased from Merck (Rahway, NJ, USA) and used without further purification. *N*-methyl-2-pyrrolidone (NMP) was chosen as the solvent for membrane preparation, while polyethylene glycol with a molecular weight of 400 g $mol^{-1}$ (PEG-400) was employed as an additive in the dope solution. PEG-400 was selected because its relatively low molecular weight can influence phase separation behavior and membrane pore formation [31,32]. In addition, its liquid form at room temperature supports convenient incorporation and homogeneous mixing in the casting solution.

Post-consumer Styrofoam, corresponding to expanded polystyrene (EPS), was collected from used food packaging waste and utilized as the primary membrane-forming material. Prior to membrane preparation, the EPS waste was cleaned to remove surface contaminants, pressed to eliminate trapped air, manually cut into small irregular pieces, and dried at ambient conditions until no visible moisture remained.

The microalgae used in this study were *Chlorella vulgaris* strains obtained from the Biorefinery Center, Universitas Gadjah Mada, Indonesia. The strains were subcultured in sterile Bold's Basal Medium (BBM). The cultures were maintained at 25 °C in an incubator with a 12-h light/12-h dark photoperiod with cool white illumination and continuous aeration using compressed air. These conditions are broadly consistent with laboratory cultivation conditions commonly reported for *Chlorella vulgaris* [33]. However, light intensity and aeration flow rate were not instrumentally monitored and therefore are not reported quantitatively. As a result, the cultivation conditions are not fully reproducible in a strict quantitative sense, although they were kept as consistent as possible throughout the experiment. In this work, the cultivation step was intended primarily to generate the feed suspension for membrane separation experiments rather than to evaluate microalgal growth kinetics or optimize cultivation conditions. Membrane preparation and related experiments were conducted under ambient laboratory conditions of approximately 22–25 °C and 45–55% relative humidity.

### Preparation of Recycled EPS Membranes

Flat-sheet recycled EPS membranes were prepared using the NIPS method. Shredded EPS waste and PEG-400 were dissolved in NMP to prepare casting solutions with varying PEG contents. The composition of each dope solution is presented in Table 1.

**Table 1.** Composition of the casting solutions used for the preparation of recycled EPS membranes with different PEG contents.

| Sample Label | EPS wt.% | PEG wt.% | NMP wt.% |
|---|---|---|---|
| EPS/PEG-0 | 20 | 0 | 80 |
| EPS/PEG-5 | 20 | 5 | 75 |
| EPS/PEG-10 | 20 | 10 | 70 |
| EPS/PEG-15 | 20 | 15 | 65 |
| EPS/PEG-20 | 20 | 20 | 60 |

The shredded EPS waste was first dissolved in NMP at 80 °C under stirring at 350 rpm for 3 h. PEG-400 was then added to the resulting EPS solution, and the mixture was stirred for a further 3 h under the same conditions to obtain a visually homogeneous casting solution. Afterward, the dope solution was degassed under vacuum for 30 min to allow entrapped air bubbles to dissipate prior to casting. The solution was cast onto a clean glass substrate. The initial film thickness was controlled using an Elcometer casting blade with a fixed gap of 100 μm.

The cast film was immediately transferred into a distilled water coagulation bath at room temperature to promote phase separation through solvent-nonsolvent exchange. The formed membranes were then transferred to fresh distilled water and soaked for 24 h to remove residual solvent before further characterization. A schematic illustration of the membrane preparation procedure is shown in Figure 1.

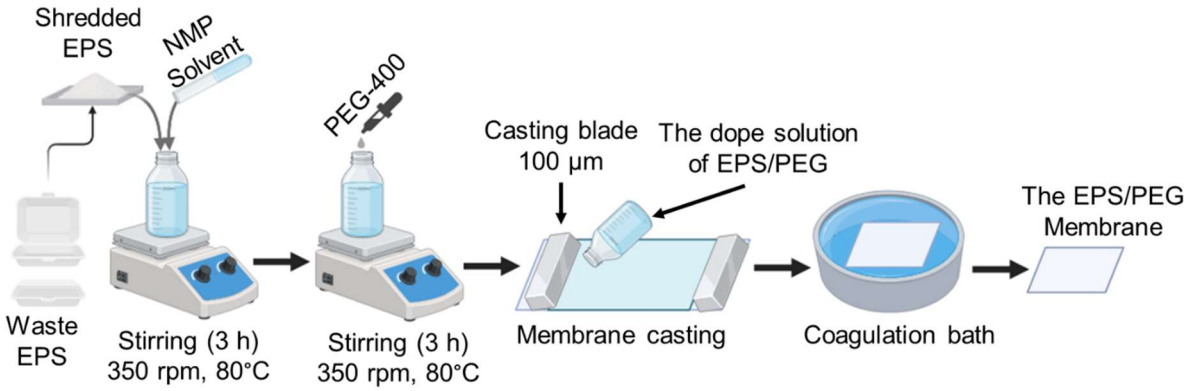


**Figure 1.** Schematic illustration of the preparation of recycled EPS/PEG flat-sheet membranes via the NIPS method.

### Membrane Characterization

The surface and cross-sectional morphologies of the prepared membranes were investigated using a scanning electron microscope (SEM) (Phenom Pro-X, Thermo Fisher Scientific, Waltham, MA, USA). Before analysis, membrane samples were dried in a vacuum oven at 80 °C for 2 h to evaporate any remaining moisture and solvent. The dried samples were cut into small pieces and sputter-coated with a thin layer of gold (~10 nm) to improve surface and image quality. For cross-sectional observation, the membrane samples were fractured in liquid nitrogen to preserve their

internal structure. SEM imaging was conducted at an accelerating voltage of 15 kV with magnifications ranging from 7500× to 15,000×. Because the working distance varied slightly among samples, it is reported directly in the corresponding SEM micrographs rather than as a single fixed value in the text.

Membrane thickness was estimated from SEM cross-sectional images using ImageJ software. For each membrane sample, measurements were taken at 10 randomly selected positions, and the average value is reported as mean ± standard deviation. Membrane porosity was determined using the gravimetric method [34]. The wet membrane was prepared by soaking the membrane in distilled water for 24 h. Surface water was carefully wiped off using clean tissue paper, and the wet weight ($W_W$) of each sample was then recorded. The samples were subsequently dried in a vacuum oven at 50 °C for 24 h, cooled at room temperature for 10 min, and weighed again to measure the dry weight ($W_d$). For each membrane formulation, three samples were analyzed and the average value was reported. The membrane porosity (ε) was calculated using Equation (1):

$$\varepsilon = \frac{W_w - W_d}{A \times l \times \rho} \times 100\% \quad (1)$$

where $A$ is the membrane surface area ($m^2$), $l$ is the membrane thickness (m), $\rho$ is the density of distilled water at 25 °C (kg $m^{-3}$) and $W_W$, $W_d$ are the wet and dry masses (kg) of the membrane sample, respectively.

The mean pore size of the membranes was estimated using the Guerout–Elford–Ferry Equation. The pore radius ($r_m$) was first calculated using Equation (2), and the reported mean pore size values correspond to the pore diameter ($2r_m$).

$$r_m = \frac{\sqrt{8\eta l Q(2.9 - 1.75\varepsilon)}}{\varepsilon A \Delta P} \quad (2)$$

where $r_m$ is the mean pore radius, $\eta$ is the viscosity of water at 25 °C (8.9 × $10^{-4}$ Pa s), $Q$ is the permeate volume per unit time ($m^3/s$), $\Delta P$ is the applied pressure (Pa), $A$ is the membrane surface area ($m^2$), $l$ is the membrane thickness (m) and $\varepsilon$ is the membrane porosity expressed as a fraction. The pore size reported in this study was taken as $2r_m$.

Membrane hydrophilicity was evaluated by water contact angle measurement using an optical goniometer (Ossila BV, Leiden, the Netherlands). A 1 µL droplet of water was placed on the membrane surface using the sessile drop method at room temperature. Due to the porous nature of the membrane, an equilibration time of 2 s was applied prior to measurement to minimize dynamic effects associated with liquid penetration into the surface pores. For each membrane, measurements were taken at three different surface locations, and the results are presented as mean ± standard deviation [35,36]. The reported values correspond to static water contact angles obtained using the sessile-drop method; advancing and receding angles were not evaluated in the present study.

Mechanical properties of the EPS membrane were evaluated using a universal testing machine (UTM) (Shimadzu EZ-LX 500N, Shimadzu Corporation, Kyoto, Japan). Membrane specimens with dimensions of 150 mm × 10 mm were mounted vertically in the testing grips with a gauge length of 100 mm and tested at a grip separation rate of 5 mm $min^{-1}$ until rupture. All measurements were performed in triplicate under the ambient conditions, and the results are reported as mean ± standard deviation. Because of the thin and porous nature of the membranes, thickness was estimated from SEM cross-sectional images rather than measured mechanically with a micrometer.

**Pure Water Flux Measurement**

The pure water flux (PWF) of the membranes was measured using a laboratory-scale dead-end filtration unit, as illustrated in Figure 2. Distilled water was used as the feed solution, and the effective membrane area was 14.6 $cm^2$. Prior to flux measurement, each membrane was compacted for 5 min at an operating pressure of 1 bar using nitrogen gas. The filtration test was then performed for 30 min under the same pressure.

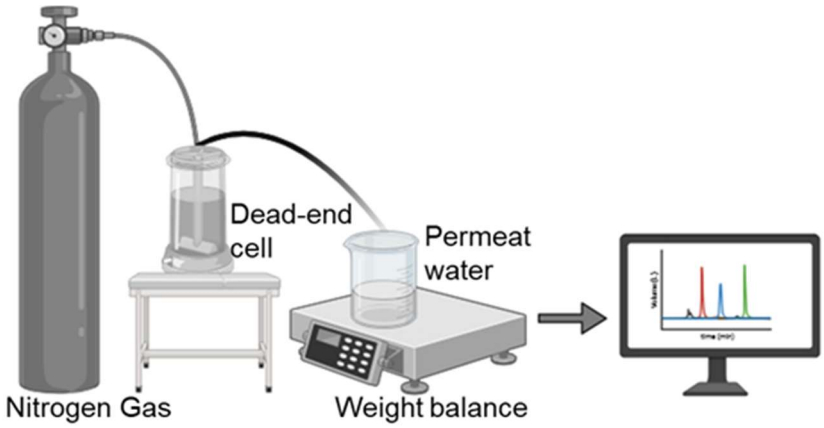


**Figure 2.** Schematic representation of the dead-end filtration setup used for PWF and microalgae separation experiments.

During filtration, the permeate mass was recorded at 60 s intervals using an electronic balance (Newtech NT-A2000, Taipei, Taiwan). Each experiment was repeated three times to ensure reproducibility, and the results are reported as mean ± standard deviation. Based on the collected permeate volume, the volumetric flux ($J_v$) and permeability flux ($L_p$) could be calculated by using Equations (3) and (4).

$$J_v = \frac{Q}{A \times \Delta t} \quad (3)$$

$$L_p = \frac{J_v}{\Delta P} \quad (4)$$

where $Q$ is the volume of permeate collected during the sampling period (in L), $\Delta t$ is the sampling time (in h), $A$ is the effective membrane area (in $m^2$), and $\Delta P$ is the applied transmembrane pressure (in bar).

### Microalgae Separation Test

Microalgae separation experiments were performed using the same dead-end filtration setup and operating conditions as those in the pure water flux test. Recycled EPS-based flat-sheet membranes were used in all experiments, and the effective membrane area was 14.6 $cm^2$. A suspension of *Chlorella vulgaris*, with a reported particle size range of 2–10 μm, was used as the feed solution. The cultivated microalgae suspension was directly used for the separation experiments, and the average turbidity of the feed was 853.94 NTU, based on repeated measurements.

A turbidity meter (Model ZD-10A, Lutron Electronic, Taipei, Taiwan) was employed to measure the turbidity of the feed and permeate solutions. The solute rejection ($R$) was calculated according to Equation (5) [37],

$$R(\%) = (1 - \frac{NTU_p}{NTU_f}) \times 100\% \quad (5)$$

where $NTU_p$ and $NTU_f$ represent the turbidity values of permeate and feed solutions of *Chlorella vulgaris*, respectively. All measurements were performed in triplicate, and the results are presented as mean ± standard deviation.

### Antifouling Performance Evaluation

The antifouling performance of the membrane was assessed through a fouling-cleaning cycle. Initially, the pure water flux ($J_{W1}$) was measured under the same operating conditions used in the microalgae separation experiment. The membrane was then subjected to microalgae separation. Following filtration, the membrane was rinsed with deionized water for 30 min to remove reversible foulant. Subsequently, the pure water flux after cleaning ($J_{W2}$) was measured under identical conditions. The flux recovery ratio ($FRR$) was determined according to Equation (6).

$$FRR\ (\%) = \frac{J_{w2}}{J_{w1}} \times 100 \quad (6)$$

where $J_{W1}$ is the initial pure water flux before microalgae filtration, and $J_{W2}$ is the pure water flux measured after membrane cleaning.

## RESULTS AND DISCUSSION

### Effect of PEG Concentration on Membrane Morphology and Structure

Figure 3 shows the top-surface morphology of recycled EPS membranes prepared at different PEG concentrations. At the magnification used, the pristine EPS membrane and the membranes containing low PEG content generally exhibit a relatively dense and smooth top-surface appearance,

as shown in Figure 3a–d. By contrast, the membrane containing 20 wt.% PEG shows more noticeable dark circular regions, which may reflect the emergence of surface pores and a tendency toward increased surface porosity [24,26]. Because the top-surface images mainly provide qualitative information on the overall surface appearance, the morphological interpretation was further supported by the cross-sectional SEM analysis (Figure 4), as well as by the contact angle and permeability results.

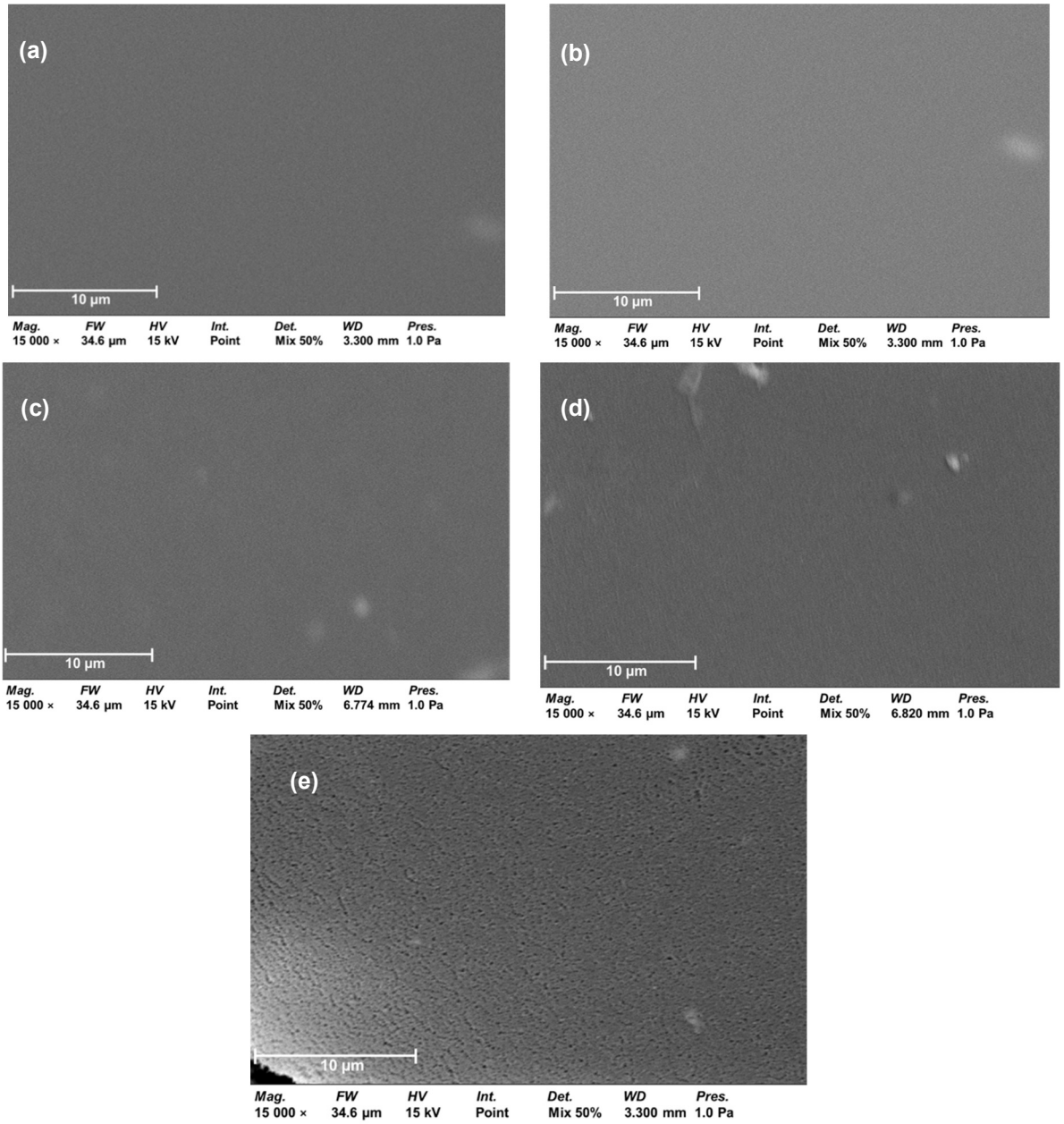


**Figure 3.** SEM surface images of the recycled EPS membranes: (**a**) pristine EPS, (**b**) EPS/PEG-5, (**c**) EPS/PEG-10, (**d**) EPS/PEG-15 and (**e**) EPS/PEG-20.

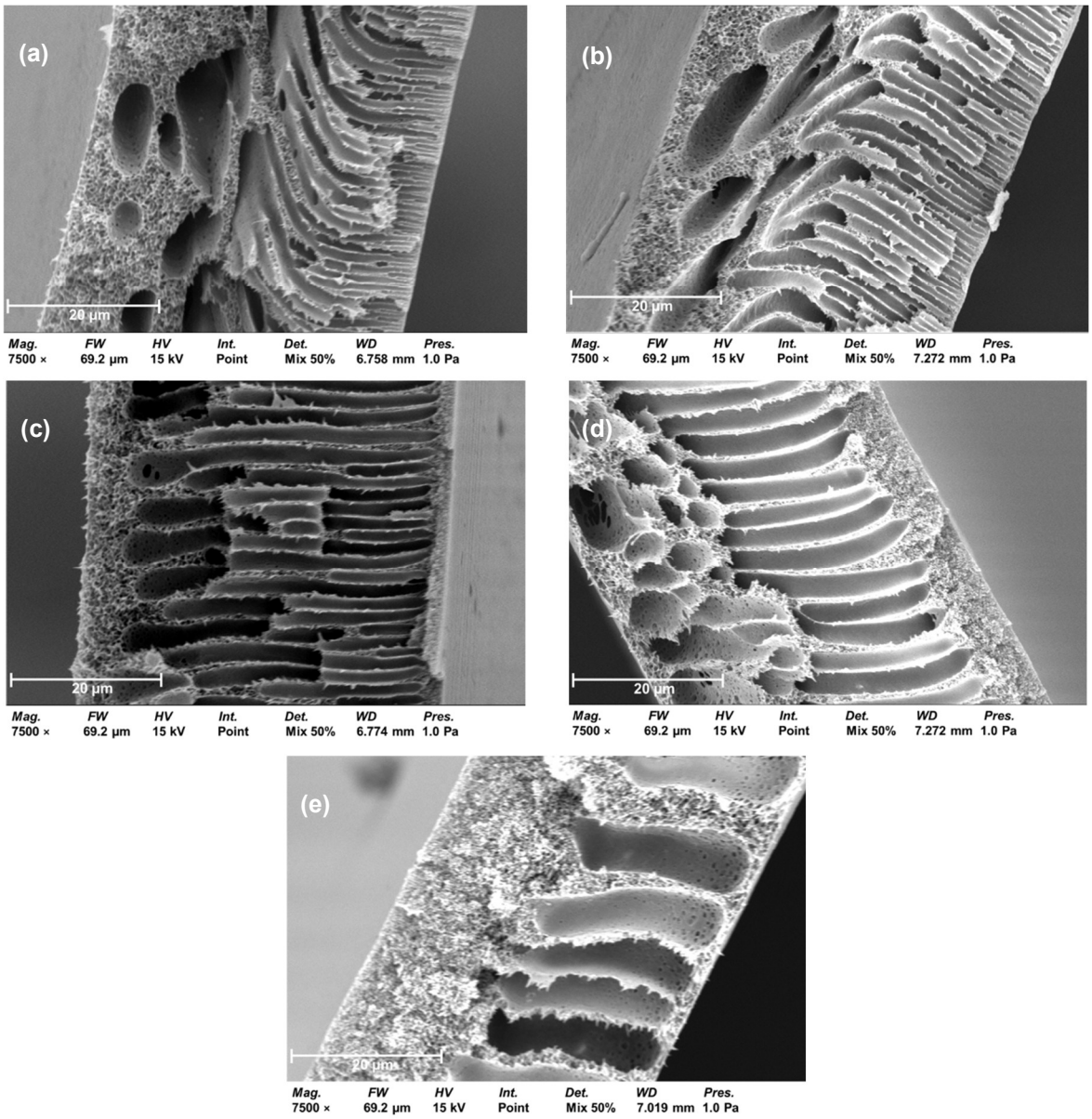


**Figure 4.** Cross-sectional SEM images of the recycled EPS membranes: (**a**) pristine EPS, (**b**) EPS/PEG-5, (**c**) EPS/PEG-10, (**d**) EPS/PEG-15 and (**e**) EPS/PEG-20.

The cross-sectional SEM images shown in Figure 4 provide clearer evidence of the structural changes induced by PEG incorporation. All membranes showed an asymmetric architecture consisting of a thin dense top layer, a finger-like intermediate region, and a more open sublayer containing macrovoids. Such an asymmetric morphology is a distinctive feature of membranes produced via phase inversion and reflects the solvent-nonsolvent exchange that occurs during immersion in the coagulation bath [38].

The incorporation of PEG appears to have influenced the phase separation behavior during membrane formation. As PEG content increased, the membranes showed progressively more pronounced finger-like structures and higher pore interconnectivity, particularly at PEG contents above 15 wt.%. This trend suggests faster demixing and more

extensive pore development in the presence of PEG. Because PEG is hydrophilic and relatively mobile in the casting solution, it likely accelerated exchange between NMP and water during immersion, thereby favoring the formation of a more open porous structure [39]. These morphological changes align with the observed increases in membrane wettability and flux.

Membrane porosity develops as the initially homogeneous polymer solution undergoes liquid-liquid demixing and solidification during phase inversion [31]. In the present system, PEG incorporation likely diminished the thermodynamic stability of the casting solution and promoted rapid phase demixing, resulting in a more porous membrane structure. As shown in Figure 4d,e, membranes containing 15–20 wt.% PEG exhibited a noticeable widening of the finger-like structures in the intermediate layer.

The membrane thickness, mean pore size, and bulk porosity of the membranes were quantified to complement the qualitative cross-sectional SEM observations, as summarized in Table 2. The prepared membranes exhibited relatively comparable thickness, ranging from 41.62 ± 0.13 μm to 48.72 ± 0.21 μm, despite the variation in PEG concentration. This indicates that the use of fixed casting-blade gap enabled reasonably consistent membrane formation. Although the overall variation in thickness was less pronounced than the changes observed in internal membrane morphology, the EPS/PEG-20 membrane notably exhibited the lowest thickness among all samples. This relatively lower thickness may have contributed to its highest pure water flux by reducing transport resistance across the membrane.

**Table 2.** Thickness, mean pore size, and bulk porosity of pristine EPS and EPS/PEG membranes.

| Sample | Thickness (μm) | Bulk Porosity (%) | Mean Pore Size (nm) |
|---|---|---|---|
| EPS/PEG-0 | 46.31 ± 0.22 | 66.7 ± 3.1 | 25.2 ± 0.9 |
| EPS/PEG-5 | 45.59 ± 0.23 | 71.4 ± 4.2 | 31.8 ± 1.6 |
| EPS/PEG-10 | 48.72 ± 0.21 | 73.2 ± 3.8 | 33.3 ± 1.5 |
| EPS/PEG-15 | 46.37 ± 0.18 | 81.0 ± 2.0 | 38.7 ± 1.0 |
| EPS/PEG-20 | 41.62 ± 0.13 | 79.9 ± 1.8 | 41.9 ± 1.0 |

In addition, both porosity and mean pore size generally increased with PEG incorporation, confirming that PEG significantly influenced pore development during phase inversion. The porosity increased from 66.7 ± 3.1% for pristine EPS to 81.0 ± 2.0% for EPS/PEG-15, followed by a slight decrease to 79.9 ± 1.8% for EPS/PEG-20. In contrast, the mean pore size increased continuously from 25.2 ± 0.9 nm for pristine EPS to 41.9 ± 1.0 nm for EPS/PEG-20. These patterns agree well with the cross-sectional SEM observations, which showed progressively more pronounced finger-like structures and greater pore interconnectivity with increasing PEG concentration.

The increase in porosity and pore size is consistent with faster solvent-nonsolvent exchange during immersion in the coagulation bath, which would favor more rapid demixing and the development of a more open porous structure. The slightly lower porosity of EPS/PEG-20 relative to EPS/PEG-15, despite its larger mean pore size, suggests that membrane permeability was governed by the combined effects of pore architecture rather than porosity alone. This is consistent with the pure water flux results, in which EPS/PEG-20 exhibited the highest flux, likely due to the simultaneous contribution of larger mean pore size, lower membrane thickness, and improved hydrophilicity. Overall, these quantitative structural data strengthen the proposed morphology–performance relationship in the PEG-modified recycled EPS membrane system.

**Surface Wettability**

The membrane wettability indicates either liquid spreading or bead formation on the material surface, hence determining its hydrophilic or hydrophobic properties [38]. In membrane filtration, the membrane surface contact angle can influence transport behavior during microalgae separation [40]. Figure 5 presents the contact angles of both pristine EPS and modified EPS/PEG membranes. The relatively high contact angle observed for the pristine EPS membrane in this research reflected the inherently hydrophobic nature of the EPS polymer.

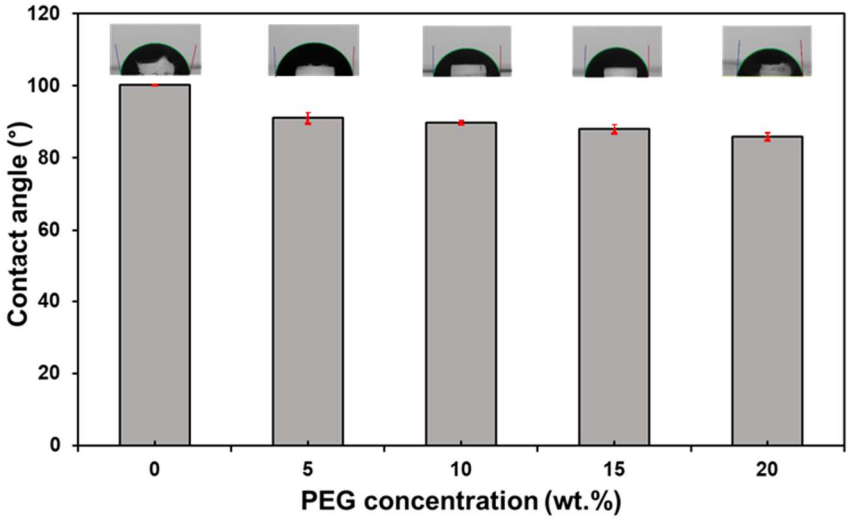


**Figure 5.** Water contact angle of pristine and PEG-modified recycled EPS membranes at different PEG concentrations.

According to the contact angle measurements, the pristine EPS membrane exhibited a water contact angle (WCA) of 100.3° ± 0.15, reflecting its relatively hydrophobic nature. By increasing PEG concentration in the EPS membrane, the contact angle gradually decreased. The EPS/PEG membrane containing 20 wt.% PEG had the lowest contact angle, at 85.94° ± 1.12, reflecting a pronounced enhancement in hydrophilicity during membrane synthesis in water. This improvement

was ascribed to the establishment of a hydration layer on the membrane top layer, promoted by the interaction between water molecules and the hydrophilic functional groups introduced by PEG [25].

The reduction in water contact angle with increasing PEG content confirms the role of PEG as a hydrophilic additive in the recycled EPS membrane system. This trend is also consistent with the structural changes observed in the membrane morphology. As shown in Table 2, PEG incorporation generally increased both membrane porosity and mean pore size, which is consistent with more extensive pore development during phase inversion. In addition, the EPS/PEG-20 membrane exhibited the lowest thickness among all samples. Together, these features suggest that PEG modification not only improved the chemical affinity of the membrane surface toward water, but also generated a more open membrane structure that facilitated water access to the porous network. Thus, the enhanced wettability of the PEG-modified membranes should be interpreted in conjunction with the accompanying structural evolution, rather than as an isolated surface phenomenon.

Such behavior agrees with the widely reported function of PEG as a hydrophilic membrane additive. Previous studies on various polymer systems, including PVDF, PVC, and polysulfone membranes, have similarly reported a decrease in contact angle following PEG incorporation, accompanied by improved surface wettability and antifouling performance [41–43]. It should be noted, however, that this comparison concerns the general trend rather than the absolute WCA values, since differences in the base polymer and membrane structure may influence the measured contact angle. Accordingly, the enhanced hydrophilicity observed in the EPS/PEG membranes is likely to be beneficial for fouling resistance, since previous studies on PEG-containing membranes have shown that improved surface wettability is commonly associated with enhanced antifouling behavior or reduced fouling tendency [39,44]. In the present study, this improved wettability is also consistent with the increase in pure water flux, particularly for EPS/PEG-20, where the combined effects of lower contact angle, larger mean pore size, and lower membrane thickness likely contributed to superior water transport.

**Mechanical Properties**

Mechanical integrity is an important requirement for membrane operation because it affects handling stability and long-term performance during filtration [45]. Figure 6 presents the tensile strength and elongation at break of pristine EPS and PEG-modified EPS membranes. Overall, PEG incorporation improved the tensile strength of the membranes relative to the pristine EPS membrane. The tensile strength increased from 0.58 ± 0.15 MPa for pristine EPS to a maximum of 1.12 ± 0.07 MPa for the membrane containing 15 wt.% PEG. This improvement may be associated with PEG-induced structural changes during phase inversion. In particular, moderate PEG incorporation promoted the development of a more open

and interconnected porous substructure, as evidenced by the SEM observations and the structural data summarized in Table 2. From EPS/PEG-0 to EPS/PEG-15, the membranes generally exhibited increasing porosity and mean pore size, indicating progressively more extensive pore development. Up to this range, the resulting membrane architecture may have facilitated more favorable stress distribution within the membrane matrix, thereby improving tensile strength. Thus, the increase in tensile strength with PEG addition should not be interpreted simply as a consequence of higher porosity, but rather as the result of structural refinement during membrane formation.

The highest tensile strength was observed for EPS/PEG-15, which also showed the highest porosity (81.0 ± 2.0%) together with a markedly increased mean pore size (38.7 ± 1.0 nm). However, a slight decline in tensile strength at EPS/PEG-20 suggests that further pore enlargement may begin to offset the beneficial effect of structural development. Although EPS/PEG-20 exhibited the largest mean pore size (41.9 ± 1.0 nm) and the lowest membrane thickness (41.62 ± 0.13 μm), the associated increase in pore openness may have introduced local stress-concentration sites within the membrane structure. These results indicate that the mechanical response of the PEG-modified membranes was governed by the balance between improved structural organization and excessive pore development at higher PEG loading.

A related trend has been reported for other additive-modified polymeric membranes. For example, the incorporation of nano-diamond-polyethylene glycol (ND-PEG) into PVC membranes improved tensile strength relative to pristine PVC, although a slight decline was observed at higher additive loading, likely due to aggregation effects [44]. This comparison supports the view that additive-assisted improvement of membrane strength depends not only on additive presence, but also on the resulting structure and the degree of pore development.

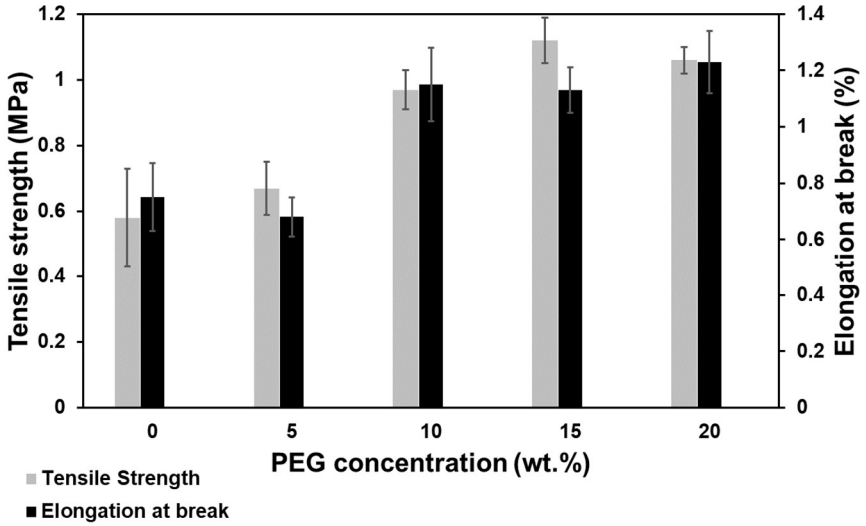


**Figure 6.** Tensile strength and elongation at break of pristine and PEG-modified recycled EPS membranes.

With respect to elongation at break, the pristine EPS membrane showed limited ductility, which is consistent with the inherently brittle nature of polystyrene-based materials [46]. The addition of 5 wt.% PEG slightly reduced elongation (from 0.7% to 0.6%), possibly due to the formation of larger finger-like pores that locally weakened the membrane structure. At 10 wt.% PEG, elongation increased markedly to 1.1%, suggesting improved chain mobility within the membrane matrix [27]. A subsequent decline at 15 wt.% PEG may be associated with the development of larger macrovoids, whereas the slight recovery observed at 20 wt.% PEG may reflect localized plasticization and polymer-chain redistribution. Overall, the variation in elongation is closely related to the morphological changes induced during phase inversion [47].

**Pure Water Flux**

Membrane filtration properties, particularly permeability and pollutant rejection, are essential for effective water treatment applications [17]. The experimental findings in this research showed a positive correlation between PEG concentration in the dope solution and PWF of the EPS/PEG membranes. As PEG content increased, PWF values rose accordingly. Specifically, the PWF of pristine EPS was 66.55 L $m^{-2}$ $h^{-1}$, which increased to 120.57, 129.98, 223.42, and 283.13 L $m^{-2}$ $h^{-1}$ for EPS/PEG-5, EPS/PEG-10, EPS/PEG-15, and EPS/PEG-20 membranes, respectively. The PWF of the prepared EPS membranes is shown in Figure 7.

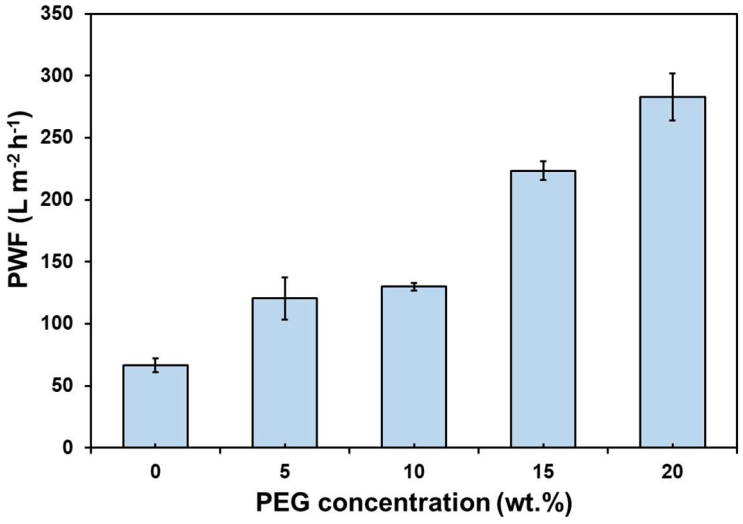


**Figure 7.** Pure water flux of pristine and PEG-modified recycled EPS membranes as a function of PEG concentration.

The increase in PWF with PEG addition can be attributed to the role of PEG as a hydrophilic pore-forming additive during membrane fabrication. PEG likely accelerated the exchange between the NMP solvent and the water nonsolvent during immersion in the coagulation bath, thereby promoting faster demixing and the development of a more open

membrane structure. This interpretation is supported by the cross-sectional SEM images (Figure 4), which show progressively more pronounced finger-like pores and greater pore interconnectivity with increasing PEG content. The structural data in Table 2 reinforce this explanation. With increasing PEG concentration, the membranes generally exhibited higher porosity and larger mean pore size, indicating more extensive pore development during phase inversion.

The porosity increased from 66.7 ± 3.1% for pristine EPS to 81.0 ± 2.0% for EPS/PEG-15, whereas the mean pore size increased continuously from 25.2 ± 0.9 nm for pristine EPS to 41.9 ± 1.0 nm for EPS/PEG-20. These data point to PEG-induced structural changes that favored water transport. At the same time, the membrane thicknesses remained within a relatively narrow range, although EPS/PEG-20 exhibited the lowest thickness (41.62 ± 0.13 μm) among all samples. This relatively lower thickness may have further reduced transport resistance across the membrane.

The increase in PWF is also consistent with the improved hydrophilicity of the membrane surface. As the PEG-modified membranes became more hydrophilic, as indicated by the decrease in water contact angle (Figure 5), the membrane surface interacted more readily with water molecules, thereby facilitating water permeation. A similar trend has been reported for other membrane systems. For example, the incorporation of 5 wt.% PEG into pristine poly(ether-ether sulfone) (PEES) membranes resulted in a flux of 233.76 L $m^{-2}$ $h^{-1}$, a contact angle of 47.46°, a water content of 70.09%, and a porosity of 30.20% [39]. At sufficiently high concentrations, however, PEG may also destabilize the casting solution and induce more substantial structural changes [26]. Previous studies have reported that excessive PEG loading can alter membrane morphology significantly and affect the resulting transport properties [31]. For this reason, PEG-400 concentrations above 20 wt.% were not investigated in the present study.

It is noteworthy that EPS/PEG-20 exhibited the highest PWF, although its porosity was slightly lower than that of EPS/PEG-15. This finding makes it clear that water permeability in the present system was not governed by porosity alone, but rather by the combined effects of mean pore size, pore architecture, membrane thickness, and surface hydrophilicity. In particular, the larger mean pore size, lower thickness, and lower water contact angle of EPS/PEG-20 likely contributed simultaneously to its superior water flux. Thus, the enhanced permeability is more reasonably attributed to the combined evolution of membrane structure and surface wettability, rather than to any single parameter in isolation.

**Microalgae Separation Performance**

The separation performance of the EPS/PEG membranes was evaluated using *Chlorella vulgaris* as the model microalgal suspension. As shown in Figure 8, all prepared membranes, including pristine EPS and PEG-modified membranes, exhibited consistently high rejection efficiencies, ranging from 99.00 ± 0.40% to 99.28 ± 0.32%. These results show that PEG

incorporation did not cause a measurable deterioration in rejection performance across the investigated formulation range.

The consistently high rejection is most consistent with a separation mechanism dominated by size exclusion, since the membrane structure remained sufficiently restrictive relative to the size of *Chlorella vulgaris* cells (approximately 2–10 μm) [48]. In this regard, membrane pore structure plays a key role in retaining microalgae while allowing water transport. PEG incorporation increased mean pore size, while porosity also increased overall with PEG addition. However, these pore sizes remained several orders of magnitude smaller than the size of the microalgal cells. Therefore, although PEG promoted a more open membrane structure and enhanced water permeation, the effective transport pathways remained far too small to permit microalgae passage [49]. This helps explain why all membranes maintained near-complete rejection despite the marked increase in permeability.

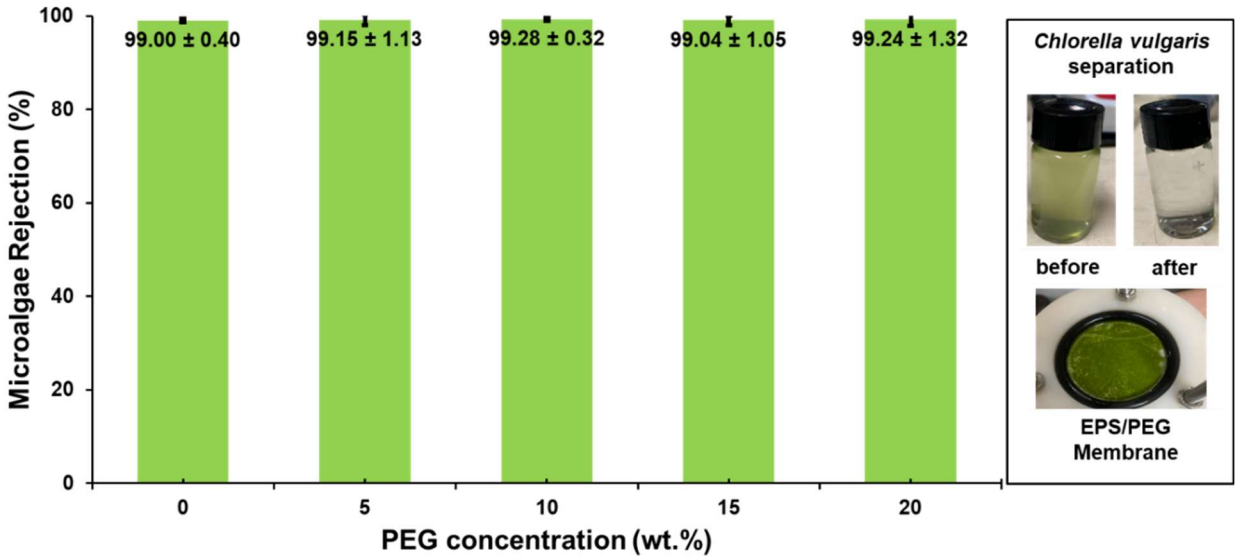


**Figure 8.** Microalgae rejection performance of pristine and PEG-modified recycled EPS membranes using *Chlorella vulgaris* as the model suspension.

The preservation of high rejection alongside increasing flux suggests that the effect of PEG in the present membrane system is better interpreted as selectivity-preserving flux enhancement, rather than as a conventional permeability–selectivity trade-off. In particular, the superior performance of EPS/PEG-20 can be understood as the result of the combined effects of larger mean pore size, relatively high porosity, lower membrane thickness, and improved hydrophilicity, all of which favored water transport without causing a measurable loss of selectivity. This interpretation is consistent with the cross-sectional SEM observations (Figure 4), which show more pronounced finger-like structures and greater pore interconnectivity at higher PEG concentrations, as well as with the added quantitative structural parameters summarized in Table 2.

Only a few EPS-based membranes reported in the literature are reasonably comparable to the present system. Fathy et al. described a cellulose acetate/EPS waste-grafted PEG composite membrane for suspended matter and salt removal, with rejection up to 99%, although the membrane matrix was primarily cellulose acetate rather than EPS [50]. Sriani et al. later explored waste EPS/polyimide flat-sheet membranes for microplastic and protein separation, showing improved selectivity and antifouling behavior, with flux around 102.3 LMH/bar and rejection above 80% for microplastics [16]. In another relevant study, Santana-Luna et al. prepared sulfonated EPS membranes for dye removal, achieving 97% rejection and a flux of 4.83 LMH for the EPS-5 membrane [51]. Within this context, the present EPS/PEG membrane appears to enhance flux while maintaining high rejection for microalgae separation, with recycled EPS serving as the principal membrane-forming component.

**Antifouling Performance**

Figure 9 presents the flux recovery ratio (FRR) of pristine EPS and EPS/PEG membranes. In general, a higher FRR reflects more effective recovery of membrane permeability after cleaning and therefore implies improved resistance to irreversible fouling [28]. Among the tested membranes, EPS/PEG-15 exhibited the highest FRR (93 ± 8.9%, which was markedly higher than that of the pristine EPS membrane (73.0 ± 2.7%), as shown in Figure 9. These results indicate that PEG incorporation generally improved the flux recovery behavior of the recycled EPS membranes.

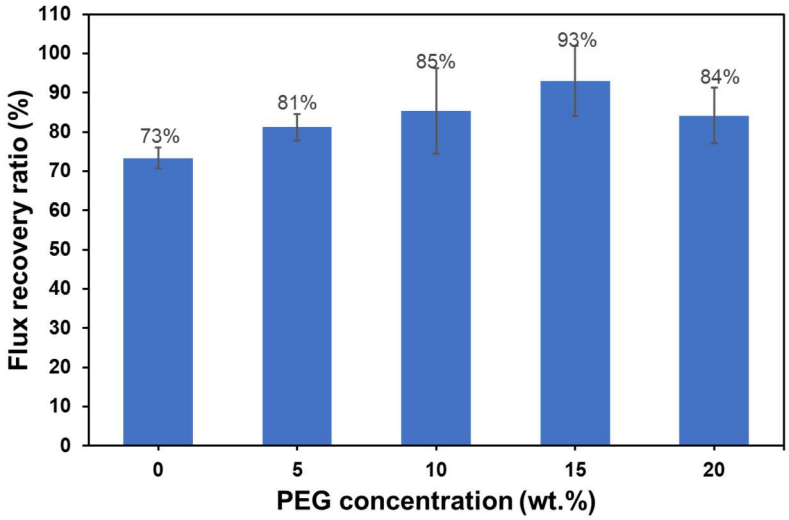


**Figure 9.** Flux recovery ratio (FRR) of pristine and PEG-modified recycled EPS membranes after microalgae filtration.

The higher FRR values obtained for the PEG-modified membranes agree with the lower water contact angle and enhanced hydrophilicity discussed earlier. A more hydrophilic membrane surface is generally less prone to strong foulant adhesion and therefore more likely to recover its

permeability after hydraulic cleaning. Although EPS/PEG-20 showed the highest pure water flux, its FRR was lower than that of EPS/PEG-15, which may indicate that the more open structure and larger pore size at higher PEG loading facilitated greater internal fouling or pore blocking during filtration. These findings highlight that the membrane formulation with the highest permeability did not necessarily provide the best fouling reversibility. Instead, antifouling behavior in the present system appears to depend on the balance between hydrophilicity, pore development, and structural compactness. Overall, the FRR results show that PEG modification improved not only membrane wettability and permeability, but also the practical filtration performance of the recycled EPS membranes, particularly at moderate PEG loading.

## CONCLUSIONS

This study demonstrates the feasibility of converting waste expanded polystyrene into flat-sheet membranes for microalgae separation through a simple NIPS-based fabrication route. PEG incorporation improved membrane hydrophilicity, altered pore development, and enhanced pure water flux, with EPS/PEG-20 showing the highest flux. The thickness, porosity, and mean pore size data confirm that PEG promoted structural changes favorable for water transport during phase inversion. Importantly, these improvements were achieved without a measurable loss of rejection, as all membranes maintained consistently high microalgae rejection (≥99%), showing that size exclusion remains the dominant separation mechanism. In addition, PEG modification improved flux recovery (*FRR*) after microalgae filtration, with EPS/PEG-15 showing the highest *FRR*, suggesting improved fouling reversibility at moderate PEG loading. Overall, the results suggest that PEG is an effective additive for improving the practical performance of recycled EPS membranes in aqueous separation. Further work should include long-term chemical and operational stability testing to better assess the suitability of these membranes for wastewater treatment applications.

## DATA AVAILABILITY

The datasets generated and analyzed during the current study are available from the corresponding author upon reasonable request.

## AUTHOR CONTRIBUTIONS

Conceptualization, MM and GSP; Methodology, GSP and NM; Formal analysis, DM and BA; Investigation, DM and INK; Visualization, INK and TS; Resources, TS; Data curation, MM, GSP and BA; Writing-original draft preparation, DM and GSP; Writing-review and editing, MM and BA; Supervision, MM, GSP and BA; Validation, TS, NM and ASB; Project administration, TS; Funding acquisition, MM, GP and ASB. All authors have read and agreed to the published version of the manuscript.

## CONFLICTS OF INTEREST

The authors declare that there are no conflicts of interest.

## FUNDING

This research is financially funded by research grant from Riset Kolaborasi Indonesia 2025: Universitas Gadjah Mada, No.1569/UN1/DITLIT/Dit-Lit/PT.01.03/2025, Universitas Airlangga, No. 1702/B/UN3.LPPM/PT.01.03/2025, Universitas Indonesia, No. PKS-636/UN2.R/HKP.05/2025.

## REFERENCES

1. Gautam B, Huang M-R, Lin C-C, Chang C-C, Chen J-T. A viable approach for polymer upcycling of polystyrene (styrofoam) wastes to produce high value predetermined organic compounds. Polym Degrad Stab. 2023;217:110528. doi: 10.1016/j.polymdegradstab.2023.110528
2. Xiang J, Song Y, Shu H, Li Z, Qiu J, Gu X. Expanded polystyrene (EPS) particles as a carrier to improve the growth of microorganisms in concrete. J Clean Prod. 2022;369:133363. doi: 10.1016/j.jclepro.2022.133363
3. Turner A. Foamed Polystyrene in the Marine Environment: Sources, Additives, Transport, Behavior, and Impacts. Environ Sci Technol. 2020;54(17):10411-20. doi: 10.1021/acs.est.0c03221
4. Elgharbawy A. Expandable polystyrene production and market survey- A review. Egypt J Chem. 2023. doi: 10.21608/ejchem.2023.137005.6041
5. Jiao T, Cao J, Zhao Y, Zhang B, Ge J, Men K, et al. From white pollution to green coating—PS/PANI anti-corrosive coatings from waste PS foams. Chem Eng J. 2024;487:150383. doi: 10.1016/j.cej.2024.150383
6. Kasar P, Sharma DK, Ahmaruzzaman M. Thermal and catalytic decomposition of waste plastics and its co-processing with petroleum residue through pyrolysis process. J Clean Prod. 2020;265:121639. doi: 10.1016/j.jclepro.2020.121639
7. Christos C, George P, Nicolas M. Comparative life cycle assessment for end-of-life treatment of expanded polystyrene produced in street markets of the municipality of Thessaloniki, Greece. Clean Technol Environ Policy. 2025;27:1953-9. doi: 10.1007/s10098-024-02930-y
8. Xie H, Li B, Lu Z, Liao Z, Li D, He L, et al. Microplastics modify the microbial-mediated carbon metabolism in mangroves. Environ Chem Lett. 2024;22:961-6. doi: 10.1007/s10311-024-01704-8
9. Bellon D, Zamudio WH, Tiria LC, Durán SM, Useche IE, Peña J. Effect of expanded polystyrene waste in the creation of waterproofing paint. J Phys Conf Ser. 2019;1386:012075. doi: 10.1088/1742-6596/1386/1/012075
10. Amariles-López CC, Aristizábal-Torres D, Alzate-Buitrago A, Osorio-Gómez CC, Mancilla-Rico E. Physicomechanical Properties of Mortar with Diluted EPS as the Binding Material. J Mater Civ Eng. 2024;36:04024414. doi: 10.1061/JMCEE7.MTENG-18010

11. Chen D, Chen M, Zhou X, Wu Y, Zhao Y, Zhang J, et al. From urban waste to environmentally friendly coating-waste cooking oil derivative/polystyrene phase change coating for foamed concrete. J Clean Prod. 2025;520:146166. doi: 10.1016/j.jclepro.2025.146166
12. Jansri E, Roungpaisan N, Pivsa-Art S, Kampeerapappun P. Sustainable Conversion of Expanded Polystyrene Waste into Nonwoven Fabric Using the Melt Jet Spinning Process: Characterization and Properties. ACS Sustain Chem Eng. 2025;13:1788-97. doi: 10.1021/acssuschemeng.4c09595
13. Sihombing YA, Sinaga MZE, Hardiyanti R, Susilawati, Saragi IR, Rangga. Preparation, characterization, and desalination study of polystyrene membrane integrated with zeolite using the electrospinning method. Heliyon. 2022;8:e10113. doi: 10.1016/j.heliyon.2022.e10113
14. Behroozi AH, Al-Shaeli M, Vatanpour V. Fabrication and modification of nanofiltration membranes by solution electrospinning technique: A review of influential factors and applications in water treatment. Desalination. 2023;558:116638. doi: 10.1016/j.desal.2023.116638
15. Rajak A, Hapidin DA, Iskandar F, Munir MM, Khairurrijal K. Electrospun nanofiber from various source of expanded polystyrene (EPS) waste and their characterization as potential air filter media. Waste Manag. 2020;103:76-86. doi: 10.1016/j.wasman.2019.12.017
16. Sriani T, Mahardika M, Miki N, Wulandari CP, Prihandana GS. Impact of polyimide on the recycling of waste expanded polystyrene into flat-sheet filtration membrane. J Mater Cycles Waste Manag. 2024;26:3745-56. doi: 10.1007/s10163-024-02073-8
17. Prihandana GS, Maulana SS, Soedirdjo RS, Tanujaya V, Pramesti DMA, Sriani T, et al. Preparation and Characterization of Polyethersulfone/Activated Carbon Composite Membranes for Water Filtration. Membranes. 2023;13:906. doi: 10.3390/membranes13120906
18. Liu S, Chu Y, Tang C, He S, Wu C. High-performance chlorinated polyvinyl chloride ultrafiltration membranes prepared by compound additives regulated non-solvent induced phase separation. J Membr Sci. 2020;612:118434. doi: 10.1016/j.memsci.2020.118434
19. Duraikkannu SL, Castro-Muñoz R, Figoli A. A review on phase-inversion technique-based polymer microsphere fabrication. Colloid Interface Sci Commun. 2021;40:100329. doi: 10.1016/j.colcom.2020.100329
20. Wu Y, Hui J, Gao S, Fan Y, Li P, Yan Z, et al. Turning waste into wealth: Bifunctional electrospun membrane based on waste expanded polystyrene for oil–water separation and anti-counterfeiting. Chem Eng J. 2025;506:160165. doi: 10.1016/j.cej.2025.160165
21. Zarghami S, Mohammadi T, Sadrzadeh M. Preparation, characterization and fouling analysis of in-air hydrophilic/underwater oleophobic bio-inspired polydopamine coated PES membranes for oily wastewater treatment. J Membr Sci. 2019;582:402-13. doi: 10.1016/j.memsci.2019.04.020

22. Gayatri R, Fizal ANS, Yuliwati E, Zailani MZ, Jaafar J, Hossain MS, et al. Effect of polyvinylidene fluoride concentration in PVDF-$TiO_2$-PVP composite membranes properties and its performance in bovine serum albumin rejection. Case Stud Chem Environ Eng. 2024;9:100620. doi: 10.1016/j.cscee.2024.100620
23. Hou C, Pang Z, Xie S, Yang Z, Wong NH, Sunarso J, et al. Dual PVP roles for preparing PVDF hollow fiber membranes with bicontinuous structures via the complex thermally induced phase separation (c-TIPS). Sep Purif Technol. 2024;332:125766. doi: 10.1016/j.seppur.2023.125766
24. Gayatri R, Fizal ANS, Yuliwati E, Hossain MS, Jaafar J, Zulkifli M, et al. Preparation and Characterization of PVDF–TiO2 Mixed-Matrix Membrane with PVP and PEG as Pore-Forming Agents for BSA Rejection. Nanomaterials. 2023;13:1023. doi: 10.3390/nano13061023
25. Khosroshahi MM, Jafarzadeh Y, Nasiri M, Khayet M. Novel polyvinyl chloride ultrafiltration membranes blended with amphiphilic polyethylene glycol-block-poly(1, 2-dichloroethylene) copolymer for oily wastewater treatment. J Water Process Eng. 2023;56:104433. doi: 10.1016/j.jwpe.2023.104433
26. Nguyen TXQ, Chen S-S, Chang H-M, Cao NDT, Singh R. Effects of polyethylene glycol and glutaraldehyde cross-linker on TFC-FO membrane performance. Environ Technol Innov. 2020;20:101059. doi: 10.1016/j.eti.2020.101059
27. Rekik SB, Gassara S, Deratani A. Green Fabrication of Sustainable Porous Chitosan/Kaolin Composite Membranes Using Polyethylene Glycol as a Porogen: Membrane Morphology and Properties. Membranes. 2023;13:378. doi: 10.3390/membranes13040378
28. Yue X, Ji X, Xu H, Yang B, Wang M, Yang Y. Performance investigation on GO-TiO2/PVDF composite ultrafiltration membrane for slightly polluted ground water treatment. Energy. 2023;273:127215. doi: 10.1016/j.energy.2023.127215
29. Ismail NQ, Azmi NA, Shoparwe NF, Ameram N, Yusoff AH. Characterization Effect of Polysulfone Membranes with Different Molecular Weight of Polyethylene Glycol Additives. IOP Conf Ser Earth Environ Sci. 2022;1102:012085. doi: 10.1088/1755-1315/1102/1/012085
30. Zhang H, Lu X, Liu Z, Ma Z, Wu S, Li Z, et al. Study of the dual role mechanism of water-soluble additive in low temperature thermally-induced phase separation. J Membr Sci. 2017;543:1-9. doi: 10.1016/j.memsci.2017.08.032
31. Zhao Z, Muylaert K, Vankelecom IFJ. Combining patterned membrane filtration and flocculation for economical microalgae harvesting. Water Res. 2021;198:117181. doi: 10.1016/j.watres.2021.117181
32. Yang K, Wang J, Zheng J, Cai W. Microalgae-based wastewater treatment: Advances and challenges in membrane harvesting technologies. Sep Purif Technol. 2025;360:130805. doi: 10.1016/j.seppur.2024.130805
33. Buriyev S, Karimova N, Rakhmatov A, Kobilov A, Qodirova S. Reproduction of chlorella (*chlorella vulgaris*) under laboratory conditions and its application in fish farming. BIO Web Conf. 2025;194:01059. doi: 10.1051/bioconf/202519401059

34. Kadanyo S, Gumbi NN, Matindi CN, Dlamini DS, Hu Y, Cui Z, et al. Enhancing compatibility and hydrophilicity of polysulfone/poly (ethylene-co-vinyl alcohol) copolymer blend ultrafiltration membranes using polyethylene glycol as hydrophilic additive and compatibilizer. Sep Purif Technol. 2022;287:120523. doi: 10.1016/j.seppur.2022.120523
35. Alfalahy HN, Al-Jubouri SM. Preparation and application of polyethersulfone ultrafiltration membrane incorporating NaX zeolite for lead ions removal from aqueous solutions. Desalination Water Treat. 2022;248:149-62. doi: 10.5004/dwt.2022.28072
36. Aryanti N, Nafiunisa A, Adina AR, Kusworo TD. Synthesis, characterization and anti-fouling properties of poly[vinylidene fluoride]-incorporated SiO2, $TiO_2$, $ZrO_2$ nanoparticle-LiCl pore former ultrafiltration membranes. Case Stud Chem Environ Eng. 2024;9:100664. doi: 10.1016/j.cscee.2024.100664
37. Al-Furaiji MH, Kalash KR, Kadhom MA, Alsalhy QF. Evaluation of polyethersulfone microfiltration membranes embedded with MCM-41 and SBA-15 particles for turbidity removal. Desalination Water Treat. 2021;215:50-9. doi: 10.5004/dwt.2021.26764
38. Saleem AG, Al-Jubouri SM. Separation performance of cationic and anionic dyes from water using polyvinylidene fluoride-based ultrafiltration membrane incorporating polyethylene glycol. Desalination Water Treat. 2024;319:100546. doi: 10.1016/j.dwt.2024.100546
39. Purushothaman M, Harikrishnan A, Senthil Kumar P, George J, Rangasamy G, Vaidyanathan VK. Enhancement of antifouling properties, metal ions and protein separation of poly(ether-ether-sulfone) ultrafiltration membranes by incorporation of poly ethylene glycol and n-ZnO. Environ Res. 2023;216:114696. doi: 10.1016/j.envres.2022.114696
40. Hashmi Z, Idriss IM, Zaini J, Abu Bakar MS, Wibisono Y, Abdullah R, et al. Advancements in membrane modifications for enhanced microalgae harvesting: A comprehensive review. Sep Purif Technol. 2025;360:131012. doi: 10.1016/j.seppur.2024.131012
41. Rajabnia H, Aroujalian A, Salimi P. Antifouling performance enhancement of PES membranes using hydrophilic nanoparticles of poly(dopamine-acrylate) for oil/water separation. J Environ Chem Eng. 2024;12:112797. doi: 10.1016/j.jece.2024.112797
42. Ren L, Deng R, Yang J, Li J, Jin J, Lei T. Improved hydrophilicity and antifouling performances of PVDF ultrafiltration membrane via in situ cross-linking. J Mater Sci. 2023;58:13854-64. doi: 10.1007/s10853-023-08879-5
43. Chen R, Mao L, Matindi CN, Liu G, He J, Cui Z, et al. Tailoring the micro-structure of PVC/SMA-g-PEG blend ultrafiltration membrane with simultaneously enhanced hydrophilicity and toughness by in situ reaction-controlled phase inversion. J Membr Sci. 2022;653:120545. doi: 10.1016/j.memsci.2022.120545
44. Shapouri L, Masoumi S, Dadgar N, Jafarzadeh Y. Preparation, characterization, and fouling analysis of PVC/ND-PEG ultrafiltration membranes for whey separation. Diam Relat Mater. 2024;142:110776. doi: 10.1016/j.diamond.2023.110776

45. Kammakakam I, Lai Z. Next-generation ultrafiltration membranes: A review of material design, properties, recent progress, and challenges. Chemosphere. 2023;316:137669. doi: 10.1016/j.chemosphere.2022.137669
46. Huang H, Huang L, Lin F, Qian W, Yin L, Xu R, et al. Room temperature brittle-to-ductile transition in polystyrene induced by extrusion casting melt stretching: Contribution of free volume and chain entanglement. Polymer. 2024;294:126745. doi: 10.1016/j.polymer.2024.126745
47. Rizqi RA, Hartono YV, Shalahuddin I, Nugroho WA, Bilad MR, Arif C, et al. Green synthesis of polyvinylidene fluoride ultrafiltration membrane with upgraded hydrophilicity. Results Mater. 2023;19:100417. doi: 10.1016/j.rinma.2023.100417
48. Ostertag F, Krolitzki E, Berensmeier S, Hinrichs J. Protein valorisation from acid whey–Screening of various micro- and ultrafiltration membranes concerning the filtration performance. Int Dairy J. 2023;146:105745. doi: 10.1016/j.idairyj.2023.105745
49. Castro-Muñoz R, García-Depraect O. Membrane-Based Harvesting Processes for Microalgae and Their Valuable-Related Molecules: A Review. Membranes. 2021;11:585. doi: 10.3390/membranes11080585
50. Fathy M, Ali HR, Moustafa YM, El Shahawy A. Removal of suspended matter and salts on ultrafiltration cellulose acetate/expanded polystyrene waste grafted PEG composite membrane. Desalination Water Treat. 2020;197:30-40. doi: 10.5004/dwt.2020.25960
51. Santana-Luna S, Yam-Cervantes M, Sulub-Sulub R, Huhn-Ibarra M, Vázquez H, Duarte S, et al. Sustainable Membranes for Water Treatment from Expanded Polystyrene Waste Using Dimethyl Isosorbide as a Green Solvent. ACS Sustain Chem Eng. 2025;13:17939-48. doi: 10.1021/acssuschemeng.5c06312

How to cite this article:
Mahmuda D, Khafifi IN, Arifvianto B, Sriani T, Prihandana GS, Baskoro AS, et al. Sustainable PEG-Incorporated Membranes Derived from Expanded Polystyrene Waste for Efficient Microalgae Separation. J Sustain Res. 2026;8(2):e260050. https://doi.org/10.20900/jsr20260050.